SwissFEL Instrument ESB
Femtosecond Pump-Probe Diffraction and Scattering

G. Ingold[1,a)], J. Rittmann[1,b)], P. Beaud[1], M. Divall[1], C. Erny[1], U. Flechsig[1], R. Follath[1], C. P. Hauri[1], S. Hunziker[1], P. Juranic[1], A. Mozzanica[1], B. Pedrini[1], L. Sala[1], L. Patthey[1], B.D. Patterson[1] and R. Abela[1,c)]

[1]*SwissFEL, Paul Scherrer Institut, 5232 Villigen PSI, Switzerland*

[a)]Corresponding author: gerhard.ingold@psi.ch
[b)]jochen.rittmann@psi.ch
[c)]URL: http://www.psi.ch/swissfel

Abstract. The ESB instrument at the SwissFEL ARAMIS hard X-ray free electron laser is designed to perform pump-probe experiments in condensed matter and material science employing photon-in and photon-out techniques. It includes a femtosecond optical laser system to generate a variety of pump beams, a X-ray optical scheme to tailor the X-ray probe beam, shot-to-shot diagnostics to monitor the X-ray intensity and arrival time, and two endstations operated at a single focus position that include multi-purpose sample environments and 2D pixel detectors for data collection.

INTRODUCTION

Combining femtosecond (fs) optical laser excitation and X-ray scattering techniques allows to study the stimulated reponse of functional crystalline materials in the time domain with atomic resolution on a sub-ps timescale. Novel electronic properties in such materials reflect a balance between several correlated interactions of long-range order, including charge and orbital ordering, magnetism, and coupling to the lattice. One way to clarify cause and effect in such coupled systems is to selectively pump and probe specific modes by tailored pulses and by tuning the system by adjusting thermodynamic variables such as temperature, magnetic field or pressure. On a sub-ps timescale the electronic and thermal response are well separated. This allows to study electronic induced switching in multiferroics and non-thermally driven non-equilibirum phase transitions to new electronic or magnetic phases in correlated electron systems by employing flexible pump and probe pulses in terms of wavelength, polarization and intensity. In a pump-probe experiment the time response - which for coherent excitation is oscillatory followed by dephasing and relaxation - is measured by precisely varying the separation between the pump and probe. Optical and THz pump pulses are derived from a fs laser system. The sample is probed by fs X-ray pulses from SwissFEL in SASE mode by time-resolved resonant and non-resonant diffraction (tr(R)XRD) and diffuse scattering (trDS), or in self-seeding mode by resonant inelastic X-ray scattering (trRIXS) in the future.

ESB INSTRUMENT

The ESB instrument [1] is operated in the energy range 4.5-12.4 keV of the fundamental. SwissFEL ARAMIS normal mode of operation is SASE in high (200 pC) and low charge (10 pC) mode [2]. At 7 keV the flux and pulse length is 1.3×10^{12} ph/s/0.1% bw & 5 fs FWHM (10 pC, 100 Hz) and 2.1×10^{13} ph/s/0.1% bw & 50 fs FWHM (200 pC, 100 Hz), respectively. Other modes of operation are the large bandwidth mode (2-4% bw), the self-seeding mode providing an order of magnitude higher spectral brightness for trRIXS, and the attosecond mode providing a fully coherent single spike with a pulse length of 0.2 fs FWHM for sub-fs experiments without crystal optics.

Proceedings of the 12th International Conference on Synchrotron Radiation Instrumentation – SRI2015
AIP Conf. Proc. 1741, 030039-1–030039-4; doi: 10.1063/1.4952862
Published by AIP Publishing. 978-0-7354-1398-6/$30.00

X-ray optics. The layout of the X-ray optics [3] is shown in Figure 1a. For pink beam a pair of bendable plane elliptical mirrors (offset mirrors, coating SiC/B_4C, Si, Mo/B_4C) installed in the optics hutch (OH) deflect the beam vertically by 6 mrad. Installed in the ESB hutch at working distance 2.5 m upstream of the endstation, a pair of bendable deflecting (8 & 12 mrad) KB-mirrors (coating Mo/B_4C) provide achromatic focusing with horizontal and vertical spot size of (1)2-200 μm FWHM for (ideal) real focusing optics.

For monochromatic beam the offset mirrors are retracted. In this case the double crystal monochromator (DCM) is the first optical element in the beam. A motorized horizontal translation allows to switch between Si(111), Si(311) and Si(511) crystal pairs. The DCM has a variable offset (20-32 mm) to optionally operate high harmonic rejection (HHR) mirrors (HHRM, coating B_4C/SiC) with variable deflection angles in a 4-bounce scheme. The beam is kept constant at height 1420 mm as for the pink beam. A HHR of $<10^{-4}$ is achieved when the fundamental is attenuated by a factor 10^2. There is the option to install diamond X-ray phase retarders (XPR) in the OH hutch downstream of DCM-HHRM. Operated in Bragg/Laue transmission geometry such XPR can provide flexible linear and circular X-rays with high degree of polarization [4, 14].

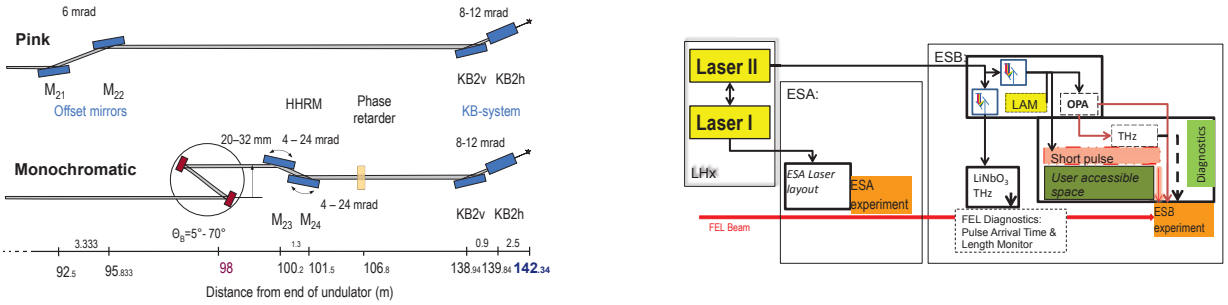

FIGURE 1. (a) Schematic layout of the X-ray optics for pink beam (top) and monochromatic beam (bottom). (b) Schematic layout of the fs laser system. Two identical lasers I, II installed in hutch LHx provide the pump-pulses for the endstations ESA and ESB.

Optical laser system. The layout of the fs optical laser system is shown Figure 1b. Two identical Ti:sapphire lasers (Laser I and II) installed in a separate laser room (LHx) serve the two endstations ESA and ESB with 20 mJ, 30 fs pulses at 100 Hz. The lasers are synchronized to the SwissFEL reference timing signal by optical fibre links stabilized below 10 fs. Each laser can be redirected to either endstation in case of laser failure. Evacuated transfer lines pass the amplified, uncompressed beam to an optical table next to the endstation where it is split in two branches, one for the pump-probe experiments and one for the X-ray timing diagnostics (XRTD). Each branch is equipped with a compressor for chirp control.

For pump-probe experiments several pumping options (UV/NIR/FIR) are available. A optical parametric amplifier (OPA) with subsequent difference frequency generation covers the spectral range 1100-15000 nm. The same output is used to generate intense THz pulses in organic crystals with field strengths exceeding 1 MV/cm [5] and pulse energy up to 10 μJ in the frequency range 1-10 THz. Very short pulses (< 10 fs) are available at 800 nm by pulse compression in a hollow core fibre [6]. To compensate for drifts in the amplifier system, a laser arrival time monitor (LAM) will be installed directly after the compressor. A variety of laser diagnostics will provide all relevant laser parameters for the user.

X-ray timing diagnostic. The XRTD-setup is installed in the ESB hutch upstream of the diamond/Si solid state attenuator (SSA). Two different techniques are used to measure the X-ray arrival time, the spectral encoding based on optical gating [7] and the photon arrival and length monitor (PALM) based on THz/IR streaking [8]. For the latter the accuracy is 0.5-5 fs rms depending on the X-ray wavelength and laser jitter. The intense THz radiation is generated by the tilted pulse front method in LiNbO3 [9]. The third method with less timing accuracy employs the X-ray arrival time derived from the electron beam arrival monitor (BAM) installed at the end of the ARAMIS undulator.

PUMP-PROBE EXPERIMENTS AND ENDSTATIONS

At SLS/FEMTO pump-probe trXRD experiments have been performed on the structural dynamics in semiconductors and semimetals, CMR manganites, CDW systems, MSMA materials, high-T_c SCs and ferroelectrics [10], and recently trRXRD experiments at the LCLS on non-equilibrium phase transition in CMR manganites [11] and on THz-induced

spin excitation in a multiferroic [12]. Using single crystals or thin film samples, the overall time resolution was 80-200 fs, depending on the experiment. At ESB such experiments are planned with time resolution < 20 fs FWHM. To achieve this in grazing incidence geometry, a X-ray focal spot size of 1-2 μm is required.

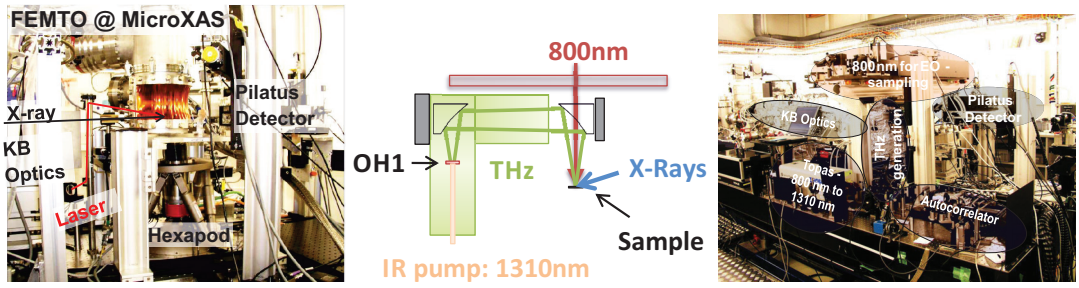

FIGURE 2. (a) FEMTO HV/UHV Cryo-chamber with cylindrical section exit window (Kapton) and 6-axes hexapod sample goniometer for laser-pump trXRD experiments. (b) Non-collinear THz-pumping scheme. (c) Setup for THz-pump/X-ray-probe diffraction experiment mounted on a single optical table including the X-ray ML-monochromator and KB-focusing optics.

R&D work. Recent work at FEMTO relevant for the ESB endstation is summarized in Figures 2a-c. An important class of experiments is trXRD in noncoplanar grazing incidence geometry where the effective probe depth can be controlled by the X-ray incidence angle (0.4°-1.5°) to match the laser (800 nm) pump depth at incidence angle ~10°. For sample temperatures in the range 100-340 K such experiments are done in ambient air using a LN_2 cryo-blower. For 20-100 K a UHV vacuum chamber ($\leq 5 \times 10^{-9}$ mbar) with a large exit window is required that allows to operate the 2D pixel detector out-vacuum. One option is a bakeable, differentially pumped double-layer Kapton window in a mountable flange (see Figure 2a), the other a welded cylindrical-section Be-window which is fixed.

A new field under rapid development is THz-pumped trXRD experiments. For hard X-rays such an experiment has recently been demonstrated at FEMTO by resonantly exciting the soft mode in a semiconductor where the THz single-cycle electric field directly drives the FE polarization [13]. The setup is shown in Figures 2b-c. Similar to the recent soft trRXRD experiment [12] at SXR/LCLS, intense THz pulses have been generated by optical rectification of IR pulses (1300-1500 nm) from an OPA in an organic crystal (OH1). A 90° non-collinear pump geometry has been chosen to combine X-ray grazing incidence with in-plane polarization of the THz electric field. In this case in comparison to collinear pumping it is more difficult to align the spatial and temporal THz/X-ray overlap via a 2-step procedure, namely THz/laser(800 nm) overlap using an EO crystal and laser(800 nm)/X-rays overlap with the sample.

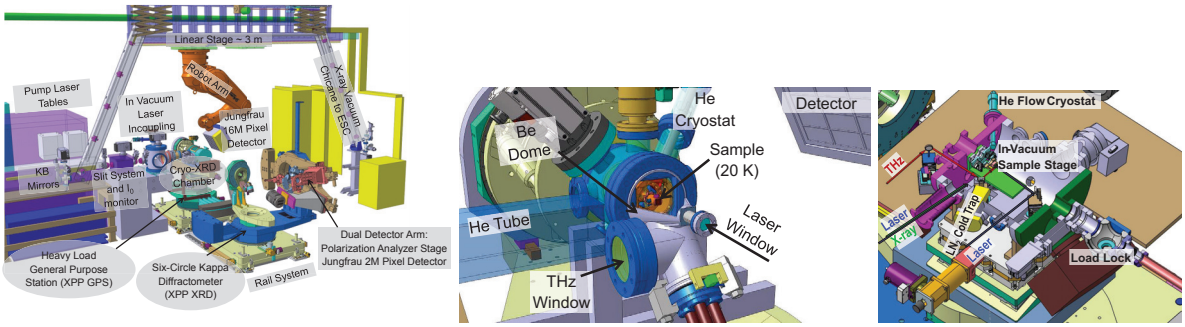

FIGURE 3. (a) ESB endstations XPP-GPS and XPP-XRD. (b) Small UHV cryo-chamber for non-collinear laser/THz-pump tr(R)XRD. (c) UHV cryo-chamber with 2-circle in-vacuum sample stage and collinear & non-collinear laser/THz pumping.

ESB endstations. The layout is shown in Figure 3a. The endstation design emphasizes rapid reconfiguration capability. There are two endstations operated at a single focal position. Mounting on rails enables convenient changeover. Sample stages designed as single modules can be swapped and mounted at both stations. Heavy load capability allows to precisely align a variety of custom built sample environmental setups including in-air goniometer stages, vacuum chambers, cryostats including DAC high pressure cells and high field magnets.

The XPP-XRD station is dedicated to X-ray pump-probe (XPP) resonant and non-resonant X-ray diffraction

(XRD) experiments. It consists of a heavy load six-circle Kappa-diffractometer with dual-detector arm carrying a 4M 2D pixel detector (Jungfrau) and a polarization analyzer stage with point detector. The Kappa-goniometer can be replaced by an open χ-circle [14] with cryostat carrier. Operated in scanning mode both in energy and momentum (reciprocal space), tr(R)XRD experiments are done for samples under a variety of environmental conditions by replacing the in-air Kappa-goniometer by custom built sample environmental modules.

The XPP-GPS station is a general purpose station (GPS) for XPP experiments in non-scanning mode. It consists of a heavy load sample goniometer and a robot detector arm carrying a 16M 2D pixel detector (Jungfrau). The Jungfrau pixel detectors are developed by the SLS detector group [15]. By swapping stages, as for XPP-XRD a variety of sample environmental modules can be accomodated. The robot detector arm is mounted to the ceiling and can be retracted up to 3 m downstream (~ 3.7 m from the focal position) to enable coherent diffraction and SAXS experiments. In this case a He flight tube between the sample and detector will be installed. For shock induced high-energy-density matter experiments the flight tube would be removed to clear space for the VISAR installation.

Until endstation ESC becomes operational, fixed target PX is initiated as a new activity at XPP-GPS [16]. A module will be developed for serial (scanning) fs crystallography at 100 Hz of 3D micro-crystals of size $< 5\,\mu$m in a cryo/in-air or He-environment. The crystals are located on a solid support (wafer), but randomly distributed. Hence a method has to be developed for in-situ crystal localization at low dose prior to the single shot diffraction scans. The portable PX-module can be mounted onto the GPS-goniometer.

Three modules are planned for trRXRD at 20 K using a He flow cryostat. First, a large HV cryo-chamber for grazing incidence and collinear laser incoupling under vacuum is shown in Figure 3a, based on the R&D work shown in Figure 2a. Second, a small UHV cryo-chamber for non-collinear laser/THz pumping is shown in Figure 3b, based on the R&D work shown in Figure 2b-c. The last THz focussing mirror is mounted close to the sample. In order not to compromise time resolution in case of a normal incident laser pulse, its intensity front will be tilted. Finally, a large UHV cryo-chamber for collinear/non-collinear laser/THz-pumping is shown in Figure 3c. A large cylindrical section Be-window is used providing access in reciprocal space of $q_{\parallel}^{max} \sim 2$ - 5 Å^{-1} and $q_{\perp}^{max} \sim 6$ - 15 Å^{-1} for 5 - 12 keV.

REFERENCES

[1] G. Ingold and P. Beaud, "SwissFEL Experimental Station B Conceptual Design Report", Paul Scherrer Institut, Switzerland, http://www.psi.ch/swissfel, (2013).
[2] SwissFEL, Paul Scherrer Institut, Switzerland, http://www.psi.ch/swissfel.
[3] R. Follath et al., (these proceedings).
[4] M. Suzuki, Y. Inubushi, M. Yabashi, and T. Ishikawa, J. Synchrotron Rad. **21**, 466-472 (2014).
[5] C. Ruchert, C. Vicario, and C.P. Hauri, Phys. Rev. Lett. **110**, 123902-1-123905-5 (2013).
[6] M. Nisoli, S. De Silvestri, and O. Svelto, Appl. Phys. Lett. **68**, 2793-2795 (1996).
[7] N. Hartmann, W. Helml, A. Galler, M.R. Bionta, J. Grünert, S.L. Molodtsov, K.R. Ferguson, S. Schorb, M.L. Swiggers, S. Carron, C. Bostedt, J.-C. Castagna, J. Bozek, J.M Glownia, D.J. Kane, A.R. Fry, W.E. White, C.P. Hauri, T. Feurer, and R.N. Coffee, Nat. Photonics **8**, 706-709 (2014).
[8] P.N. Juranic, A. Stepanov, R. Ischebeck, V. Schlott, C. Pradervand, L. Patthey, M. Radovic, I. Gorgisyan, L. Rivkin, C.P. Hauri, B. Monoszlai, R. Ivanov, P. Peier, J. Liu, T. Togashi, S. Owada, K. Ogawa, T. Katayama, M. Yabashi, and R. Abela, Opt. Express **22**, 30004-30012 (2014).
[9] J. Hebling, G. Almasi, I.Z. Kozma, J. Kuhl, Opt. Express **10**, 1161-1166 (2002).
[10] FEMTO, Paul Scherrer Institut, Switzerland, http://www.psi.ch/femto.
[11] P. Beaud, A. Caviezel, S.O. Mariager, L. Rettig, G. Ingold, C. Dornes, S.-W. Huang, J.A. Johnson, M. Radovic, T. Huber, T. Kubacka, A. Ferrer, H.T. Lemke, M. Chollet, D. Zhu, J.M. Glownia, M. Sikorski, A. Robert, H. Wadati, M. Nakamura, M. Kawasaki, Y. Tokura, S.L. Johnson, and U. Staub, Nat. Materials **13**, 923-927 (2014).
[12] T. Kubacka, J.A. Johnson, M.C. Hoffmann, C. Vicario, S. de Jong, P. Beaud, S. Grübel, S.-W. Huang, L. Huber, L. Patthey, Y.-D. Chuang, J.J. Turner, G.L. Dakovski, W.-S. Lee, M.P. Minitti, W. Schlotter, R.G. Moore, C.P. Hauri, S.M. Koohpayeh, V. Scagnoli, G. Ingold, S.L. Johnson, U. Staub, Science **343** 1333-1336 (2014).
[13] S. Grübel et al., (in preparation).
[14] J. Strempfer, S. Francoual, D. Reuther, D.K. Shukla, A. Skaugen, H. Schulte-Schrepping, T. Kracht and H. Franz, J. Synchrotron Rad. **20**, 541-549 (2013).
[15] SLS Detector Group, Paul Scherrer Institut, Switzerland, http://www.psi.ch/detectors.
[16] B. Pedrini, (private communication).